arXiv:1301.3107v1 [cond-mat.str-el] 14 Jan 2013

Anomalous enhancement of the Wilson ratio in a quantum spin liquid: $Na_4Ir_3O_8$

Gang Chen[1, *] and Yong Baek Kim[2]
[1]Department of Physics, University of Colorado, Boulder, CO, 80309-0390, U.S.A.
[2]Department of Physics, University of Toronto, Toronto, Ontario M5S 1A7, Canada

(Dated: January 15, 2013)

We present a theory for recent experiments on the quantum spin liquid candidate material $Na_4Ir_3O_8$. In particular, we provide an explanation of large enhancement and high sensitivity of the Wilson ratio and magnetic susceptibility across the metal-insulator transition (MIT). We consider an extended Hubbard model on a hyperkagome lattice, which incorporates atomic spin-orbit coupling (SOC) and multi-orbital interactions of Ir 5d electrons. We analyze the model near MIT and study thermodynamic properties across the MIT. We propose that the system on the insulating side is a U(1) quantum spin liquid with spinon Fermi surfaces. We further show that, the magnetic susceptibility experiences multiple enhancements from the strong SOC, reduced bandwidth and onsite spin-orbital exchange, while the heat capacity does not. Understanding of the currently available experiments and suggestions for future experiments are discussed.

PACS numbers: 75.10.Jm, 71.27.+a

Quantum spin liquid (QSL) is an exotic state of matter with fractionalized excitations and emergent gauge fields. QSLs on the theoretical side are well established, but it has been very challenging to identify the direct evidence for the existence of QSLs in real materials. Recently, however, several materials have been proposed as promising candidates of QSL[1]. While no magnetic ordering has been observed in these systems, there exist thermodynamic signatures indicating the presence of gapless spin-carrying excitations with a finite charge excitation gap. One natural explanation of these spin-carrying excitations would be spinons in QSL phases. The central question in the context of QSLs, therefore, is what kind of spin liquid phases may be realized in these systems.

In this work, we present a theory of a three-dimensional QSL that may be realized in $Na_4Ir_3O_8$, an Ir-based hyperkagome lattice system. We focus on recent experiments of anomalously enhanced Wilson ratio across the metal-insulator transition (MIT) in this material. Using a semi-realistic model of Ir t_{2g} orbitals, it is shown that the anomalously large Wilson ratio is a natural consequence of the QSL phase arising from strong spin-orbit coupling (SOC) and multi-orbital interactions. Combined with other spin liquid phenomenology, such a large Wilson ratio would be a fingerprint of a *spin-orbital QSL*, where the spinons have both spin and orbital characters.

In the early experiment on polycrystalline $Na_4Ir_3O_8$ samples in Ref. 2, the magnetic susceptibility and heat capacity did not show any signature of magnetic ordering down to the lowest measurable temperature. NMR Knight shift measurement further confirms the absence of magnetic ordering down to 2K[3]. With the Curie-Weiss tempeature $\Theta_{CW} = -650$K, the frustration parameter (defined as $f \equiv \frac{\Theta_{CW}}{T_N}$ with T_N the ordering temperature) is greater than 300. Moreover, in the zero temperature limit, the magnetic susceptibility saturates to a finite and large constant while the heat capacity has a linear temperature dependence with a rather small coefficient γ ($\gamma \equiv \frac{C_v}{T}$). This leads to an anomalously large Wilson ratio $W \equiv \frac{\pi^2}{3}\frac{\chi/\mu_B^2}{\gamma/k_B^2}$ at low temperature, that equals to 35 ! Most of other promising QSL candidate materials have a Wilson ratio of order of unity at low temperatures [1]. In particular, the organic materials such as κ-(BEDT-TTF)$_2$Cu$_2$(CN)$_3$[4] and EtMe$_3$Sb[Pd(dmit)$_2$]$_2$[5] also show constant magnetic susceptibility and linear-in-temperature heat capacity, often taken as an evidence for spinon Fermi surface. These materials are close to a MIT and it has been suggested that a QSL phase of spinon Fermi surfaces may arise upon gapping out charge excitations via a second order transition starting from the metallic side[6, 7]. In this case, the spinon Fermi surface would be a remnant of the electron Fermi surface and the Wilson ratio would not change much across MIT. While $Na_4Ir_3O_8$ may also be close to a MIT due to the extended nature Ir *d*-orbitals, a simple extension of this argument would not explain the large Wilson ratio. Clearly, a different or an additional physics is at work for $Na_4Ir_3O_8$.

Recently there have been new experiments on single crystal samples[3]. Depending on the preparation, the single crystal samples can be both insulating and metallic. Comparing the most conducting metallic sample and the insulating polycrystalline sample, one finds that, the heat capacity only has a very small change with γ varied by 17% while the magnetic susceptibility is increased by a factor of 7. In general, for the single crystal samples, the magnetic susceptibility is much more sensitive to MIT than the heat capacity, and is strongly enhanced on the insulating side.

There have been several theoretical proposals about the nature of the disordered state on the insulating side[8–11]. It should be pointed out that all of the existing proposals have assumed a spin-1/2 Heisenberg model on a hyperkagome lattice. Ref. 10 suggested a U(1)

QSL with spinon Fermi surfaces based on a projective wavefunction study. Such a state is certainly qualitatively consistent with the Fermi-liquid-like phenomenology in $\mathrm{Na_4Ir_3O_8}$. The Wilson ratio in this proposal, however, should still be order of unity because of the spin-rotational invariance. Ref. 9 introduced a $\mathrm{Z_2}$ QSL with spinon pairing. They attribute the large Wislon ratio to the suppression of the heat capacity by the spinon pairing. Even though the singlet spinon pairing also suppresses the magnetic susceptibility, they argue that this can be avoided if SOC energy scale is greater than the pairing strength. This state, if relevant for $\mathrm{Na_4Ir_3O_8}$, may indicate emergent superconductivity for the metallic samples at similar temperature scales. If there is no superconductivity, the metallic samples are expected to have a much larger heat capacity than the insulating ones. Neither is observed in the recent experiments[3].

Although the ground state of the Heisenberg model on the hyperkagome lattice itself is an interesting theoretical problem, the applicability of this model to the actual material can only be justified in the strong Mott regime with certain assumptions[12]. In fact, both the polycrystalline sample and single crystal samples are proximate to a MIT. We also notice that all other QSL candidate materials can be modelled by either a single-band Hubbard model in an intermediate or the strong Mott regime. On the other hand, in $\mathrm{Na_4Ir_3O_8}$, all the three t_{2g} orbitals are involved and hence the electron interactions are orbitally dependent. Moreover, since Ir is a heavy element, a large SOC is naturally expected[12]. An important question is which aspects of these ingredients give rise to qualitatively different thermodynamic behaviors.

In this paper, we analyze the extended Hubbard model on the Ir-based hyperkagome lattice, including all the three t_{2g} orbitals, SOC, and the electron interactions on these orbitals. We assume that the MIT is controlled by the correlation. We separate the multi-orbital interactions into the Hubbard-U interaction for the charge sector and the onsite spin-orbital exchange for the spin-orbital sector. We study the MIT in this model by a slave-rotor mean-field theory. The main result of this paper is that, the strong SOC and the correlation both suppresses the electron bandwidth, which effectively enhances the onsite spin-orbital exchange in the insulating side. SOC breaks the spin-rotational symmetry and enhances the bare electron/spinon magnetic susceptibility, and the magnetic susceptibility is further enhanced by the "enhanced" onsite spin-orbital exchange. While the spin suceptibility gets multiple enhancements, the heat capacity is only sensitive to the density of state on the Fermi surface which does not experience strong enhancement. This leads to a large enhancement in the Wilson ratio across the MIT.

To write down our model, we make use of a few well-known facts about the microscopics related to $\mathrm{Na_4Ir_3O_8}$[12] The local $\mathrm{IrO_6}$ crystal field first splits the 5d electron states into a low-lying t_{2g} triplet and a much higher e_g doublet which will play no role. The atomic SOC acts on the three t_{2g} orbitals. Moreover, there may also exist further crystal field splitting among the three t_{2g} orbitals that arises from the small distortion of the $\mathrm{IrO_6}$ octahedron[2]. Including the hopping of electrons, the non-interacting part of the Hamiltonian is given by

$$\begin{aligned}\mathcal{H}_0 = &\sum_{i,mn,\alpha\beta} \frac{\lambda}{2}\mathbf{L}_{mn}\cdot\boldsymbol{\sigma}_{\alpha\beta} d^\dagger_{im\alpha} d_{in\beta} + \sum_{i,m,\alpha} D_{im} d^\dagger_{im\alpha} d_{im\alpha} \\ &+ \sum_{\langle ij\rangle,mn,\alpha} t_{ij,mn} d^\dagger_{im\alpha} d_{jn\alpha}. \end{aligned} \tag{1}$$

Here $d_{im\alpha}$ describes the electron with orbital $m = xy, yz, xz$ and spin $\alpha = \uparrow,\downarrow$ at site i, and $\mathbf{L}$ ($\boldsymbol{\sigma}$) is the orbital angular momentum (spin Pauli matrix). In Eq. (1), the single-ion anisotropy D_{im} captures the distortion of the $\mathrm{IrO_6}$ octahedra. For the hopping, we include both direct and oxygen p-orbital mediated indirect electron tunneling. The details about different terms in $\mathcal{H}_0$ are further discussed in the supplementary material[13].

For the interaction, we adopt the standard multi-orbital interaction that includes intra-orbital repulsion (U), inter-orbital repulsion (U'), Hund's coupling (J) and pairing hopping (J'),

$$\begin{aligned}\mathcal{H}_I = &U\sum_{i,m} n_{im\uparrow}n_{im\downarrow} + \frac{U'}{2}\sum_{i,m\neq m'} n_{im}n_{im'} \\ &+ \frac{J}{2}\sum_{i,m\neq m',\sigma\sigma'} d^\dagger_{im\sigma} d^\dagger_{im'\sigma'} d_{im\sigma'} d_{im'\sigma} \\ &+ \frac{J'}{2}\sum_{i,m\neq m'} d^\dagger_{im\uparrow} d^\dagger_{im\downarrow} d_{im'\downarrow} d_{im'\uparrow}. \end{aligned} \tag{2}$$

Here, $n_{im\alpha} = d^\dagger_{im\alpha} d_{im\alpha}$ and $n_{im} = \sum_\alpha d^\dagger_{im\alpha} d_{im\alpha}$. In the atomic limit, these four Kanamori's parameters in Eq. (2) have the relation $U = U' + J + J'$, $J = J'$, which is assumed in the following discussion. Such a multi-orbital interaction is certainly very complicated to deal with. To manifest the physics, we follow the treatment in Ref. 14 and decompose this multi-orbital interaction into the charge part $\mathcal{H}_c$ and the spin-orbital part $\mathcal{H}_{ex}$ with $\mathcal{H}_I = \mathcal{H}_c + \mathcal{H}_{ex}$ and

$$\begin{aligned}\mathcal{H}_c = &\frac{U}{2}\sum_i (n_i - 5)^2 , \\ \mathcal{H}_{ex} = &-J\sum_{i,m\neq m'} n_{im}n_{im'} + \frac{J}{2}\sum_{i,m\neq m'} d^\dagger_{im\uparrow} d^\dagger_{im\downarrow} d_{im'\downarrow} d_{im'\uparrow} \\ &+ \frac{J}{2}\sum_{i,m\neq m',\sigma\sigma'} d^\dagger_{im\sigma} d^\dagger_{im'\sigma'} d_{im\sigma'} d_{im'\sigma}. \end{aligned} \tag{3}$$

Here, we assume the average electron occupation per site is 5, appropriate for the Ir^{4+} ion with $5\mathrm{d}^5$ electron configuration. We neglect an unimportant constant in $\mathcal{H}_c$. $\mathcal{H}_c$ is the usual Hubbard-U interaction and describes the energy cost for the electron charge fluctuation. $\mathcal{H}_{ex}$ describes how the electrons arranges themselves among different spin-orbital states, i.e. onsite spin-orbital exchange interaction. Since $\mathcal{H}_c$ and $\mathcal{H}_{ex}$ describe two different physics, we will treat them separately.

The Hubbard U is the largest energy scale in the interaction and is treated in the first place. We first consider the Hamiltonian $\tilde{\mathcal{H}} = \mathcal{H}_0 + \mathcal{H}_c$ and analyze the phase diagram within the slave-rotor mean-field treatment[15]. In the slave-rotor formalism, we decompose the electron operator into a bosonic charge rotor $e^{i\theta_i}$ and a fermionic spinon $f_{im\alpha}$ (that carries spin and orbital quantum numbers), i.e. $d_{im\alpha} \equiv e^{-i\theta_i} f_{im\alpha}$. With this decomposition, the physical Hilbert space is enlarged and we need to impose a constraint $L_i = \sum_{m\alpha} f^\dagger_{im\alpha} f_{im\alpha} - 5$ to get back to the physical Hilbert space. Here, L_i is the angular momentum operator conjugate with θ_i, $[\theta_i, L_j] = i\delta_{ij}$. The Hamiltonian $\tilde{\mathcal{H}}$ expressed in the rotor and spinon variables is further decomposed into two mean-field Hamiltonians for the rotors and the spinons, respectively,

$$\mathcal{H}_r = \frac{U}{2}\sum_i (L_i^2 + hL_i) + Q_r \sum_{\langle ij\rangle} e^{i(\theta_i - \theta_j)} \tag{4}$$

$$\mathcal{H}_f = \sum_{i,mn,\alpha\beta} \frac{\lambda}{2} \mathbf{L}_{mn} \cdot \boldsymbol{\sigma}_{\alpha\beta} f^\dagger_{im\alpha} f_{in\beta} + \sum_{i,m,\alpha} D_{im} f^\dagger_{im\alpha} f_{im\alpha} + Q_f \sum_{\langle ij\rangle,mn,\alpha} t_{ij,mn} f^\dagger_{im\alpha} f_{jn\alpha} - h \sum_{i,m,\sigma} f^\dagger_{im\sigma} f_{im\sigma}. \tag{5}$$

Here, h is the Langrange multiplier introduced to implement the constraint on average, and the mean field parameters Q_r and Q_f are given by $Q_r \equiv \sum_{mn\sigma} t_{ij,mn} \langle f^\dagger_{im\sigma} f_{jn\sigma}\rangle_f$ and $Q_f \equiv \langle e^{i(\theta_i - \theta_j)}\rangle_r$, where the subindices indicate the mean field ground state to evaluate over. Here we have made a uniform mean field approximation such that Q_f and Q_r are uniform on all the bonds and the ground state is smoothly connected to the non-interacting case. When the rotor is condensed with $\langle e^{i\theta_i}\rangle \neq 0$, the spinon binds with the charge rotor, form an electron with a finite quasi-particle weight $Z \neq 0$, and the system is in a Fermi liquid phase. When the rotor is uncondensed with $\langle e^{i\theta_i}\rangle = 0$, the spinons are deconfined, form spinon Fermi surfaces, and the system is in a U(1) QSL phase. We solve this mean-field Hamiltonians self-consistely. The rotor condensation is signaled when the lowest rotor mode turns gapless.

In the phase diagram depicted in Fig. 1, there are three different energy scales: SOC, correlation and bandwidth. SOC narrows the electron bandwidth, which effectively enhances the correlation effect and drives a MIT at a reduced critical interaction. This is the key underlying reason for the presence of strong correlation physics in 5d electron systems[16] which were long believed to be weakly correlated. Moreover, the correlation also suppresses the bandwidth and thus enhances SOC effect.

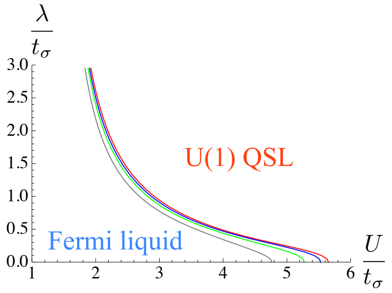

FIG. 1. (Color online) The slave-rotor mean-field phase diagram[17] with the Hubbard-U in the charge sector only. t_σ is the σ-bonding hopping amplitude[13]. Different curves corresponds to different single-ion anisotropy parameter D. From left to right, $D = 0.8t_\sigma, 0.4t_\sigma, 0.2t_\sigma, 0$.

Using Ioffe and Larkin's relation[18], we have for the heat capacity $C_v = C_{vf} + C_{vr}$ with C_{vf} (C_{vr}) the spinon's (rotor's) contribution. Since the rotor's contribution is subdominant at low temperatures, $C_{vr} \propto T^3$ in the Fermi liquid phase, $C_{vr} \propto e^{-\Delta/T}$ (Δ is the charge gap) in the Mott insulator, we then have $C_v \approx C_{vf}$. The magnetic susceptibility comes only from the spinon's contribution, i.e. $\chi = \chi_f$. In the slave-rotor formalism for the Hamiltonian $\tilde{\mathcal{H}}$, the spinons are essentially treated as free fermions. In Fig. 2, we have computed the thermodynamic quantities for two different SOCs ($\lambda = 0.8t_\sigma, t_\sigma$) with $D = 0$ and $D = 0.2t_\sigma$. The specific heat is not monotonic because the spinon/electron Fermi surface changes due to the presence of the anisotropy and the SOC. The specific heat with $D = 0$ only varies slightly near the MIT, which is consistent with the experiments. Taking $t_\sigma = 0.64$eV and $\lambda = t_\sigma = 0.64$eV[19], we find $\gamma \approx 3.63$mJ/molK^2, only slight larger than the experimental value ($\approx$3mJ/molK^2)[3]. The specific heat with $D = 0.2t_\sigma$ is strongly suppressed near the MIT in contrast to the experiments. This suggests the actual material may not have a strong anistropy due to the IrO$_6$ distortion. In Fig. 2, we only find a small enhancement of magnetic susceptibility, which is inconsistent with the experiments. Since the Wilson ratio is sensitive to magnetic fluctuations, and moreover, it is the magnetic susceptibility that varies significantly in the experiments, we naturally turn to the onsite spin-orbital exchange $\mathcal{H}_{ex}$ that has not been so far included in our analysis.

We follow Ref. 14 and place the onsite exchange $\mathcal{H}_{ex}$ into the spinon mean-field Hamiltonian $\mathcal{H}_f$ and treat the $\mathcal{H}_{ex}$ by a weak coupling analysis. This treatment is justified by the fact that $\mathcal{H}_{ex}$ describes the spin-orbital exchange rather than the charge fluctuation. Moreover, to further assist this treatment, we also take the exchange coupling to be much weaker than the Hubbard U interaction. The new spinon mean-field Hamiltonian $\mathcal{H}_{fn}$ is given by $\mathcal{H}_{fn} = \mathcal{H}_f + \mathcal{H}_{ex}$ with $\mathcal{H}_{ex}$ expressed in terms of spinon operators. Since the ground state does not have magnetic order, the inclusion of the exchange into

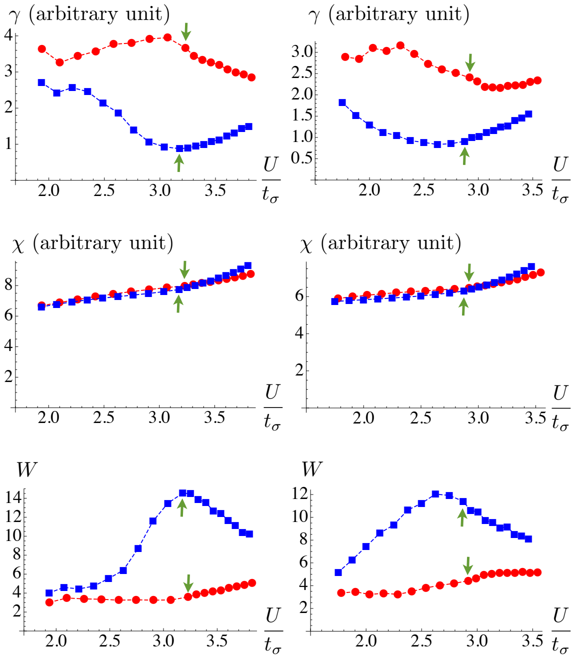

FIG. 2. (Color online) The specific heat, susceptibility and Wilson ratio obtained from slave-rotor mean-field theory with the Hubbard-U in the charge sector only. In the left (right) three plots, we have $\lambda = 0.8t_\sigma$ ($\lambda = t_\sigma$). In all the plots, the red circular (blue squared) dots are data points with $D = 0$ ($D = 0.2t_\sigma$). Dashed curves connecting the dots are for guidance. The arrows indicate the location for metal-insulator transition. The results are obtained for a finite system with $40 \times 40 \times 40$ unit cells at $T = 0.0005t_\sigma$.

the spinon Hamiltonian does not modify the mean-field phase diagram in a weak coupling approach. Moreover, the density of state on the Fermi surface is not modified by the inclusion of the exchange, so the heat capacity stays invariant as the case without the exchange.

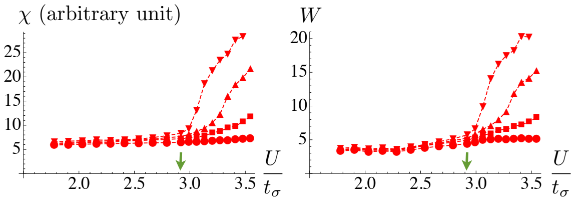

FIG. 3. (Color online) Magnetic susceptibilities and Wilson ratios for $\lambda = t_\sigma, D = 0$, including the spin-orbital exchange. In both plots, from top to bottom, $J = 0.3t_\sigma, 0.2t_\sigma, 0.1t_\sigma, 0$. Dashed curves connecting the dots are for guidance. The arrows indicate the location for metal-insulator transition. The results are obtained for a finite system with $40 \times 40 \times 40$ unit cells at $T = 0.0005t_\sigma$.

The magnetic susceptibility can be strongly enhanced by this onsite spin-orbital exchange. Because the spin-rotational symmetry is explicitly broken by the SOC and the orbital angular momentum also contributes to the magnetization, the magnetic susceptibility is not just sensitive to density of state at the Fermi surface but is sensitive to the whole many-body states. This is quite different from a normal Fermi liquid with spin-rotation invariance. The onsite spin-orbital exchange favors the electrons to occupy different orbitals and thus increase the orbital angular momentum. Note that putting electrons onto a single orbital state tends to quench the orbital angular momentum. The orbital angular momentum further couples to the spin via SOC. The presence of spin-orbital exchange strongly modifies the system's response to external magnetic fields.

The resulting magnetic susceptibilities and Wilson ratios with different spin-orbital exchange are plotted in Fig. 3. The magnetic susceptibility is only slightly enhanced by the exchange on the Fermi liquid side, while it is strongly enhanced on the QSL side. Here two relevant energy scales are the electron bandwidth and the exchange. In the Fermi liquid phase, the bandwidth is broad and a weak exchange does not cause much change. In the QSL phase, the bandwidth is suppressed by the correlation and SOC, which effectively enhances the onsite exchange. The enhanced onsite spin-orbital exchange, together with the SOC, leads to a large enhancement of magnetic susceptibilities and Wilson ratios.

Here we discuss additional experimental probes to detect the QSL in $Na_4Ir_3O_8$. It is known that Ir absorbs neutron which prevents neutron scattering measurement for small size samples. A recently developed experimental technique, resonant inelastic X-ray scattering, can overcome this difficulty in iridates and may provide an opportunity to observe the spinon continuum in the low-energy spin sector[20]. Transport measurement such as thermal conductivity may also provide an indirect evidence for the spinon Fermi surfaces if a metal like behavior is observed[21].

To summarize, we propose that the ground state in the insulating $Na_4Ir_3O_8$ is a U(1) quantum spin liquid with spinon Fermi surfaces. We show that the anomalously large enhancement and high sensitivitiy of the Wilson ratio across the metal-insulator transition is due to the combined effects of strong SOC, correlation and onsite spin-orbital exchange.

We thank L. Balents, P. A. Lee and D. Podolsky for helpful discussions. We expecially thank R. Perry and H. Takagi for sharing their experimental data before publishing. GC was supported by DOE award no. de-sc0003910. YBK was supported by the NSERC, CIFAR, and Centre for Quantum Materials at the University of Toronto. Some of this work was carried out at the Kavli Institute for Theoretical Physics; our stays there were supported by NSF grant no. PHY11-25915.

---

[*] email address: gang.chen@colorado.edu

[1] L. Balents, Nature **464**, 199 (Mar 2010)
[2] Y. Okamoto, M. Nohara, H. Aruga-Katori, and H. Takagi, Phys. Rev. Lett. **99**, 137207 (Sep 2007)
[3] R. Perry and H. Takagi, Private communication
[4] Y. Kurosaki, Y. Shimizu, K. Miyagawa, K. Kanoda, and G. Saito, Phys. Rev. Lett. **95**, 177001 (Oct 2005)
[5] T. Itou, A. Oyamada, S. Maegawa, M. Tamura, and R. Kato, Phys. Rev. B **77**, 104413 (Mar 2008)
[6] T. Senthil, Phys. Rev. B **78**, 045109 (Jul 2008)
[7] D. Podolsky, A. Paramekanti, Y. B. Kim, and T. Senthil, Phys. Rev. Lett. **102**, 186401 (May 2009)
[8] M. J. Lawler, H.-Y. Kee, Y. B. Kim, and A. Vishwanath, Phys. Rev. Lett. **100**, 227201 (Jun 2008)
[9] Y. Zhou, P. A. Lee, T.-K. Ng, and F.-C. Zhang, Phys. Rev. Lett. **101**, 197201 (Nov 2008)
[10] M. J. Lawler, A. Paramekanti, Y. B. Kim, and L. Balents, Phys. Rev. Lett. **101**, 197202 (Nov 2008)
[11] E. J. Bergholtz, A. M. Läuchli, and R. Moessner, Phys. Rev. Lett. **105**, 237202 (Dec 2010)
[12] G. Chen and L. Balents, Phys. Rev. B **78**, 094403 (Sep 2008)
[13] See the supplementary material for the details of the non-interacting Hamiltonian.
[14] W.-H. Ko and P. A. Lee, Phys. Rev. B **83**, 134515 (Apr 2011)
[15] S. Florens and A. Georges, Phys. Rev. B **70**, 035114 (Jul 2004)
[16] D. Pesin and L. Balents, Nature Physics **6**, 376 (March 2010)
[17] We follow Ref.15 and double the critical correlation U_c at MIT to keep the right atomic limit.
[18] L. B. Ioffe and A. I. Larkin, Phys. Rev. B **39**, 8988 (May 1989)
[19] M. R. Norman and T. Micklitz, Phys. Rev. B **81**, 024428 (Jan 2010)
[20] B. J. Kim, H. Ohsumi, T. Komesu, S. Sakai, T. Morita, H. Takagi, and T. Arima, Science **323**, 1329 (Mar. 2009)
[21] Y. Minoru, N. Nakata, Y. Senshu, M. Nagata, H. Yamamoto, R. Kato, T. Shibauchi, and Y. Matsuda, Science **328**, 1246 (June 2010)

SUPPLEMENTARY MATERIAL

Non-interacting Hamiltonian

As shown in Fig. 4, the Ir hyperkagome lattice has 12 sublattices in the unit cell. Each IrO$_6$ is slightly distorted and generates a single-ion anisotropy in the Hamiltonian $\mathcal{H}_0$. At each Ir site, there exists a 2-fold rotational axis and the symmetry-allowed single-ion anisotropy has several independent terms. We pick up a term that is likely to be the dominant single-ion anisotropy. For instance, the anisotropy at sublattice 4 in Fig. 4 is given by $\sum_{mn,\sigma} D[(l^z)^2]_{mn} d^\dagger_{im\sigma} d_{in\sigma}$, where $\mathbf{l}_{mn} = \mathbf{L}_{mn}$ and $D > 0$. Anisotropies on other sublattices can be readily obtained by symmetry.

Our tight-binding model contains three parameters: σ-bonding t_σ and π-bonding t_π for direct electron tunneling, and t_{id} hopping for the indirect electron tunneling through the intermediate oxygen p-orbitals. We neglect the higher-order processes involving the tunneling between two different oxygen p-orbitals. For instance, the hopping Hamiltonian between sublattice 4 and 5 is of the form,

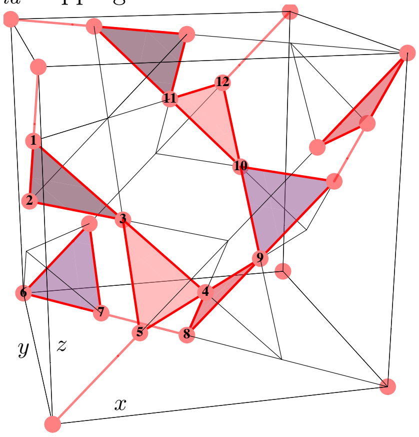

FIG. 4. (Color online) Ir based hyperkagome lattice and its parent pyrochlore lattice. "1,2,$\cdots$,12" label the 12 sublattices. Solid bonds (in red) connect Ir sites.

$$\begin{aligned}\mathcal{H}^{45}_{hop} = \sum_{\alpha} & t_{id}(d^\dagger_{i,xz,\alpha} d_{j,yz,\alpha} + d^\dagger_{i,yz,\alpha} d_{j,xz,\alpha}) \\ & + \frac{t_\pi}{2}(d^\dagger_{i,xz,\alpha} - d^\dagger_{i,yz,\alpha})(d_{j,xz,\alpha} - d_{j,yz,\alpha}) \\ & - t_\sigma d^\dagger_{i,xy,\alpha} d_{j,xy,\alpha} + h.c. \qquad (6)\end{aligned}$$

In this paper, we choose $t_\pi/t_\sigma = 0.1$ and $t_{id}/t_\sigma = 0.6$ that are close to the ones used in the band structure calculation in Ref.19 of the main text.